ACS Sustainable Chemistry & Engineering

pubs.acs.org/journal/ascecg

Research Article

Access to Biorenewable and CO_2-Based Polycarbonates from Exovinylene Cyclic Carbonates

Fabiana Siragusa, Elias Van Den Broeck, Connie Ocando, Alejandro J. Müller, Gilles De Smet, Bert U. W. Maes, Julien De Winter, Veronique Van Speybroeck,* Bruno Grignard,* and Christophe Detrembleur*

Cite This: https://dx.doi.org/10.1021/acssuschemeng.0c07683

Read Online

ACCESS | Metrics & More | Article Recommendations | Supporting Information

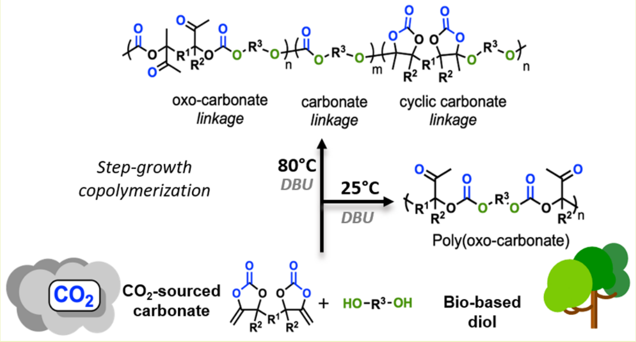

ABSTRACT: We investigate the scope of the organocatalyzed step-growth copolymerization of CO_2-sourced exovinylene bicyclic carbonates with bio-based diols into polycarbonates. A series of regioregular poly(oxo-carbonate)s were prepared from sugar- (1,4-butanediol and isosorbide) or lignin-derived (1,4-benzenedimethanol and 1,4-cyclohexanediol) diols at 25 °C with 1,8-diazabicyclo[5.4.0]undec-7-ene (DBU) as a catalyst, and their defect-free structure was confirmed by nuclear magnetic resonance spectroscopy studies. Their characterization by differential scanning calorimetry and wide-angle X-ray scattering showed that most of them were able to crystallize. When the polymerizations were carried out at 80 °C, some structural defects were introduced within the polycarbonate chains, which limited the polymer molar mass. Model reactions were carried out to understand the influence of the structure of alcohols, the temperature (25 or 80 °C), and the use of DBU on the rate of alcoholysis of the carbonate and on the product/linkage selectivity. A full mechanistic understanding was given by means of static- and dynamic-based density functional theory (DFT) calculations showing the determining role of DBU in the stability of intermediates, and its important role in the rate-determining steps is revealed. Furthermore, the origin of side reactions observed at 80 °C was discussed and rationalized by DFT modeling. As impressive diversified bio-based diols are accessible on a large scale and at low cost, this process of valorization of carbon dioxide gives new perspectives on the sustainable production of bioplastics under mild conditions.

KEYWORDS: *polycarbonate, carbon dioxide valorization, alkylidene cyclic carbonate, bio-based diols, organocatalysis, thermal properties, DFT modeling, molecular dynamics*

■ INTRODUCTION

Polycarbonates (PCs) are widely used in the automotive industry and in the electric/electronic or construction sectors. Their unique features derived from their excellent physical properties such as high thermal stability and impact resistance combined with their excellent transparency make them suitable for organic glasses, optical fibers, resistant packaging, and so forth.[1,2] PCs are industrially manufactured by phosgenation of diols. The corrosive and highly toxic phosgene combined with the quest for polymers with reduced carbon footprint pushed the scientific community and industries to engineer novel synthetic pathways for this important polymer family.[3,4] Among the numerous processes currently investigated for producing PCs, merging carbon dioxide (CO_2) as a safe and renewable substitute to phosgene with bio-based diols appeared as a promising and appealing approach for greener PCs.[5−7] Indeed, the recent developments in biorefineries (e.g., lignin fractionation and sugar fermentation techniques) have contributed to diversify the range of bio-based alcohols and polyols that can be exploited for the production of more sustainable materials.[8,9] Although the direct copolymerization of (bio-based) diols with CO_2 is highly attractive for the preparation of PCs by an alternative phosgene-free route, this process currently remains very challenging due to the difficulty in removal of water during the polycondensation (Scheme 1a). The rare examples showed that only low molar mass PCs (M_n < 5000 g/mol) were collected using a high loading of metal oxides[10] or organocatalyst/desiccant dual systems at high temperatures, with a limited substrate scope.[6] Another attractive approach to merge CO_2 and diols for the production

Received: October 19, 2020
Revised: December 10, 2020

Scheme 1. Synthesis of PCs by Copolymerization of Diols with CO_2 or CO_2-Sourced Building Blocks: (a) Direct Dehydrative Polycondensation of Diols with CO_2; (b) Melt Polycondensation of Acyclic Carbonates Prepared by the Dehydrative Coupling of CO_2 with Alcohols and Diols; (c) Organocatalyzed Step-Growth Copolymerization of CO_2-Sourced Exovinylene Bicyclic Carbonates with Bio-Based Diols; and (d) Step-Growth Copolymerization of bisαCCs Obtained from Epoxides, CO_2, and 1,4-Butynediol

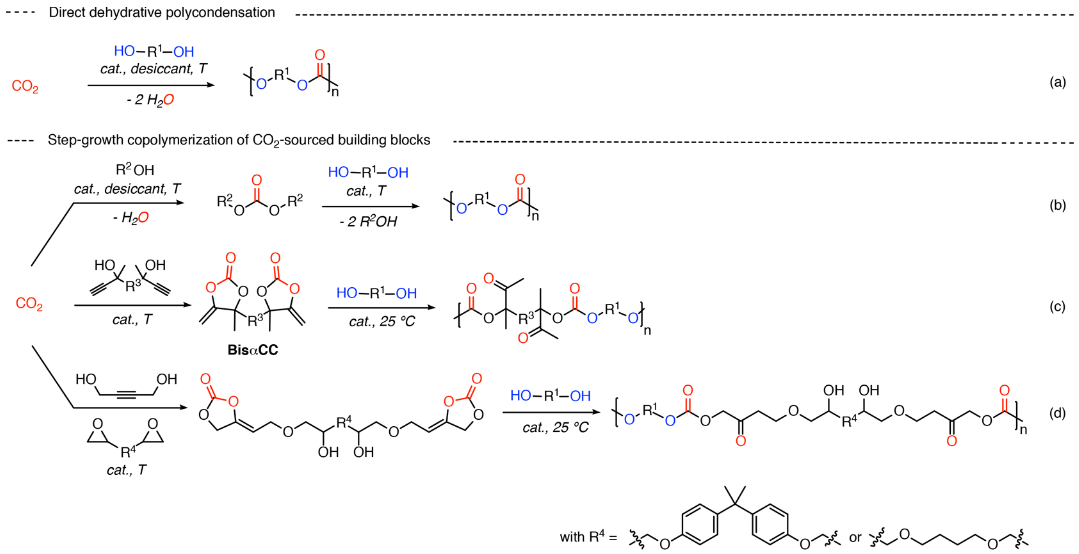

of a larger range of PCs consists of the melt polycondensation of acyclic dialkyl- (e.g., dimethyl carbonate) or diaryl-carbonates (e.g., diphenyl carbonate) with diols. The dialkyl-/diaryl-carbonates were prepared by the dehydrative coupling of CO_2 with the corresponding alcohols (Scheme 1b). Polycondensation is often carried out in a multistage process involving the fabrication of oligomers at moderate temperatures (T = 80−120 °C), followed by applying a high vacuum at higher temperatures (T > 200 °C) to remove the volatile byproducts (methanol or phenol) and pushing the reaction toward the formation of polymers of higher molar mass.[11−14] Recently, our group pioneered the exploitation of a novel family of CO_2-based monomers [bis(α-alkylidene carbonate)s, bisαCCs] for the facile construction of PCs by the organocatalyzed step-growth copolymerization with diols under mild reaction conditions (Scheme 1c).[15,16] The presence of an exovinylene group on the five-membered cyclic carbonate moiety significantly enhanced its reactivity with alcohols and controlled the regioselective ring-opening producing regioregular functional poly(oxo-carbonate)s (PCs) at room temperature up to reasonable molar masses (M_n = 17,000 g/mol). These novel monomers were produced by the zinc iodide-catalyzed carboxylative coupling of CO_2 to bis(propargylic alcohol)s. BisαCCs were also able to copolymerize with amines to produce new polyurethanes[15,17,18] or with thiols to provide novel sulfur-containing polymers, that is, polythiocarbonates and poly(cyclic carbonate-*co*-thioether)s.[19] Although this family of CO_2-sourced monomers was highlighted by BASF[20] as promising building blocks for the preparation of CO_2-based polymers, their utilization for PC synthesis is still in its infancy. In 2019, we exploited bisαCCs for chain-extending poly(ethylene glycol) (PEG) diols and producing poly(carbonate-*co*-ether)s that found promising application as solid electrolytes in Li-ion batteries.[16] The same concept adapted to a mixture of PEG diol and a dithiol enabled the production of new poly(carbonate-*co*-(thio)ether)s containing both linear and cyclic carbonate linkages within the polymer backbone that demonstrated some utility for battery applications.[21] Very recently, Schaub et al. designed new bisαCCs from 1,4-butynediol, epoxides, and CO_2 and successfully tailored low molar mass poly(β-oxo-carbonates) by polyaddition with 1,4-butanediol (Scheme 1d).[22] *In situ*-formed bisαCCs could also be polymerized by an organocatalyzed cascade reaction between a bispropargylic alcohol, CO_2, and a diol. However, only low molar mass polymers (M_n < 3000 g/mol) were collected due to the occurrence of side-reactions.[23] Hitherto, only linear aliphatic primary diols (i.e., 1,4-butanediol or PEG diol) were copolymerized with preformed bisαCCs until achieving reasonable molar masses, whereas the reactivity of bisαCCs toward biorenewable alcohols of different chemical structures remains unknown. Understanding the copolymerization features while identifying the limitations of bisαCC chemistry is key to enlarge the scope of PCs that could be produced by this appealing process.

In this work, we demonstrate that combining bisαCCs with various bio-based diols derived from sugar[24−26] or lignin[8,9] diversifies the range of regioregular PCs that can be produced (Scheme 1c). We investigate the influence of the alcohol structure [i.e., (cyclo)aliphatic or aromatic] and the temperature on the polymerization features, PC microstructure, molar mass, and their thermal properties. Kinetic studies carried out on model compounds combined with modeling also enable us to understand the formation of some unexpected linkages in the polymer chain. This study demonstrates that a large scope of functional CO_2 and bio-sourced polymers with a high biorenewable content can be easily produced by this new process, potentially enlarging the application range of PCs.

■ EXPERIMENTAL SECTION

Materials and Methods. Benzyl alcohol (99%), 1-butanol (98%), and cyclohexanol were purchased from Sigma-Aldrich. 1,4-Butanediol (99%), 1,4-cyclohexanediol (99%), and *trans*-1,4-cyclohexanediol were supplied by Fluorochem, while 1,8-diazabicyclo[5.4.0]undec-7-ene (DBU 99%) and 1,4-benzenedimethanol (99%) were purchased from TCI. 4,4-Dimethyl-5-methylene-1,3-dioxolan-2-one (αCC), 4,4′-(ethane-1,2-diyl)bis(4-methyl-5-methylene-1,3-dioxolan-2-one (C1), 1,9-dimethylene-2,4,10,12-tetraoxodispiro[4.2.4^{8}.2^{5}]-tetradecane-3,11-dione (C2) and tetrabutylammonium phenolate were synthesized, as reported elsewhere by our group.[15,19,27] All solid reagents were dried before use with azeotropic distillations in toluene. All the solvents were dried overnight on activated 3 Å molecular sieves. All the reactions were performed under an inert atmosphere of N_2.

Characterization Methods. *Nuclear Magnetic Resonance Spectroscopy.* ^{1}H nuclear magnetic resonance (NMR) analyses were performed on Bruker 400 MHz spectrometers in DMSO or $CDCl_3$ at 25 °C in the Fourier-transform mode. 16 or 64 scans for ^{1}H spectra and 512 or 2048 scans for ^{13}C spectra were recorded. Cross-polarization magic-angle spinning solid-state ^{13}C NMR spectra were collected using a Bruker AVANCE DSX-400 instrument. Samples were packed in 4 mm zirconia rotors and spun at 10 kHz.

Gas Chromatography−Mass Spectrometry. Samples were prepared by taking 100 μL of the compound mixture and diluting in acetone. The sample was filtered over a syringe filter and further diluted to a concentration of 10^{-4} to 10^{-5} M. 3 μL of the samples were injected. The apparatus used was an Agilent Technologies 7890 A GC System coupled to an Agilent Technologies 5975 C inert MSD with a triple-axis detector. As the column, an Optima 725820.30 30 m × 250 μm × 0.25 μm was selected. The carrier gas was helium. The following oven program was used: first 50 °C for 3 min, then increment of 10 °C/min up to 300 °C, followed by 300 °C for 5 min. The front inlet was heated at 200 °C. Mass was scanned from 50 to 450 amu.

Size Exclusion Chromatography. The number-average molecular weight (M_n), weight-average molecular weight (M_w), and molecular-weight dispersity (M_w/M_n) values of polymers were determined by size exclusion chromatography (SEC) in dimethylformamide (DMF) and in chloroform ($CHCl_3$). The SEC in DMF contained LiBr (0.025 M) and was performed at 55 °C (flow rate: 1 mL/min) with a Waters chromatograph equipped with three columns (Waters Styragel PSS gram 1000 Å (×2), 30 Å), a dual λ absorbance detector (Waters 2487), and a refractive index detector (Waters 2414). The SEC in chloroform was performed at 35 °C at a flow rate of 1 $cm^3 \cdot min^{-1}$, using an isocratic pump (VE 1122, Viscotek), a set of two PLgel 5 μm MIXED-C ultrahigh efficiency columns, and a Shodex SE 61 differential refractive index detector and a variable wavelength UV detector (Spectra 100, Spectra-Physics). A volume of 100 μL of sample solution in chloroform (concentration, 0.3% w/v) was injected. Polystyrene standards (Polymer Laboratories) with narrow molecular weight distributions were used to generate a calibration curve.

Positive-Ion Matrix-Assisted LASER Desorption/Ionization-Mass Spectrometry. Positive-ion matrix-assisted LASER desorption/ionization-mass spectrometry (MALDI-MS) experiments were performed using a Waters QToF Premier mass spectrometer equipped with a Nd:YAG laser operating at 355 nm (third harmonic) with a maximum output of 65 μJ delivered to the sample in 2.2 ns pulses at 50 Hz repeating rate. Time-of-flight mass analysis was performed in the reflectron mode at a resolution of about 10k (m/z 569). All samples were analyzed using *trans*-2-[3-(4-*tert*-butylphenyl)-2-methylprop-2-enylidene]malononitrile as a matrix. Polymer samples were dissolved in $CHCl_3$ to obtain 1 $mg \cdot mL^{-1}$ solution. Additionally, 40 μL of 2 $mg \cdot mL^{-1}$ NaI solution in acetonitrile was added to the polymer solution.

Thermogravimetric Analysis. Thermogravimetric analysis (TGA) was performed on a TGA2 instrument from Mettler Toledo. Approximately 5 mg of sample was heated at 20 °C/min until 600 °C under a N_2 atmosphere (20 mL/min).

Differential Scanning Calorimetry. Differential scanning calorimetry (DSC) was performed on a DSC Q2000 differential calorimeter (TA Instruments). All the experiments were performed under ultrapure nitrogen flow. Samples of 5−8 mg were used and placed in sealed aluminum pans. The samples were first heated at a rate of 10 °C min^{-1} from 25 to 150 °C. Subsequently, the samples were cooled down to −80 °C at a rate of 10 °C min^{-1} and then heated to 230 °C at 10 °C min^{-1}. The last heating cycle was used for the determination of T_g.

Flash Differential Scanning Calorimetry. Flash differential scanning calorimetry (FDSC) was performed on a Flash DSC2+ instrument from Mettler Toledo, equipped with a Huber TC-100 intracooler. The cooling rate employed was −4000 K/s, and the heating rates were 1000, 5000, and 20,000 K/s. Applying a very fast cooling rate (−4000 K/s), most samples were quenched to the amorphous state (or their crystallinity was greatly reduced), thereby facilitating the detection of their glass transition upon subsequent heating at 1000 K/s. Second, the use of fast heating rates permits avoiding cold crystallization of the samples. For the detection of the melting temperature, a cooling rate of −0.1 K/s was also employed in order to induce crystallization of the samples at −80 °C from the melted state before the subsequent heating scan at 5000 K/s. The polymers with higher values of T_m were evaluated at a heating rate of 20,000 K/s to avoid the degradation of the sample. Before each experiment, the sensor was conditioned and calibrated. A flow of nitrogen gas was applied to perform the measurements under an inert atmosphere, maintaining an 80 mL/min flow rate. For a good contact between the sample and the sensor, a fluorinated oil was casted over the sensor and then the sample was loaded. This oil does not show thermal transitions in the temperature range under study. The samples were analyzed in a range from −80 to 200 or 350 °C, depending on the thermal degradation temperature of each polymer determined by TGA. The reported values of T_g and T_m were taken from the heating runs. As the mass employed in fast chip calorimeter experiments is so small, the results are assumed to be independent of sample mass. STARe software was used to analyze the data.

Wide-Angle X-ray Scattering. Wide-angle X-ray scattering (WAXS) X-ray powder diffraction patterns were collected using a Philips X'pert PRO automatic diffractometer operating at 40 kV and 40 mA, in a θ−θ configuration, using a secondary monochromator with Cu-Kα radiation (λ = 1.5418 Å) and a PIXcel solid state detector (active length in 2θ 3.347°). Data were collected from 5 to 70° 2θ, with a step size of 0.026° and a time per step of 150 s at RT. A 1° fixed soller slit and a divergence slit giving a constant volume of sample illumination were used.

General Procedure for the Model Reaction of αCC with Alcohols. All model reactions were conducted at 25 °C with an equimolar ratio of αCC and the nucleophile in dry DMSO (C = 4 mol/L) under a N_2 atmosphere. Kinetics were monitored by ^{1}H NMR spectroscopy following the representative procedure for the αCC−alcohol reaction: αCC (4 mmol 1 equiv) and alcohol (4 mmol 1 equiv) were added in a reaction tube with 1 mL of dry DMSO and 5 mol % DBU (0.2 mmol) compared to αCC. Samples were taken after different time intervals and analyzed by ^{1}H NMR spectroscopy to determine the αCC conversion.

General Procedure for the Synthesis of Poly(β-oxo-carbonate)s. The representative procedure for the synthesis of PCs: C1 (3.93 mmol, 1 g) and 1,4-benzenedimethanol (3.93 mmol, 0.542 g) were added to a flask and then dry DMSO (5 mL) and DBU (0.196 mmol, 0.03 mL) were added under nitrogen at room temperature (25 °C). The reaction medium was then stirred at 25 °C for 24 h. At the end of the reaction, an aliquot was withdrawn to determine the conversion of monomers by ^{1}H NMR spectroscopy. The polymer was purified by precipitation in methanol/water (1:1). The polymer was then dried under vacuum at 25 °C for 48 h and analyzed by ^{1}H- and ^{13}C-NMR spectroscopy and SEC. The same procedure was carried out for the other polymers.

■ RESULTS AND DISCUSSION

Prior to considering the polymerizations, we first carried out a series of reactions on model compounds. The objective of these studies was to probe the reactivity of the α-alkylidene cyclic carbonate group with alcohols of various structures that mimic bio-based alcohols that will be used later in polymerization (Scheme 2). The main goal was to identify the optimal conditions for high yields and selectivity and to investigate the

Scheme 2. Model Compounds Mimicking the Structure of Sugar- and Lignin-Based Monomers

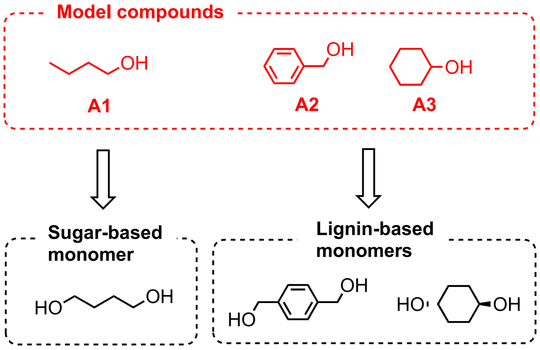

influence of the temperature on the process. Although the temperature was expected to accelerate the reactions, it might also promote some side reactions that have to be identified as they can have an impact on the polymer microstructure and molar masses. These model reactions are therefore of prime importance for understanding the polymerization processes that will be studied.

Alcoholysis of Exovinylene Cyclic Carbonate via Model Reactions. αCC (Figure 1a) was selected as the model cyclic carbonate and synthesized by the quantitative carboxylative coupling of CO_2 to 2-methyl-3-butyn-2-ol catalyzed by tetrabutyl ammonium phenolate.[27] Three alcohols, 1-butanol (**A1**), cyclohexanol (**A2**), and benzyl alcohol (**A3**), were selected based on their structural similarities with sugar- or lignin-based diols (Scheme 2) that will be involved later in the polymerizations. Butanol was also used as a benchmark for the sake of comparison with the two other alcohols.

The reactions were first realized at 25 °C under stoichiometric conditions using dry DMSO as a solvent. These stoichiometric conditions between αCC and the alcohol were selected to fit the conditions required for a step-growth polymerization that will be implemented later. As expected, no alcoholysis of αCC was observed even after 24 h for all alcohols in the absence of catalyst. The addition of 1,5-diazabicyclo(5.4.0)undec-7-ene (DBU) (5 mol % compared to αCC) was then considered as it was previously shown to catalyze the ring-opening of α-alkylidene cyclic carbonates with primary aliphatic alcohols.[15] Under these conditions, the oxo-carbonate adducts were selectively and quantitatively formed (>99% yield) after 24 h of reaction (Figure 1a). The rates of ring-opening reactions by different alcohols were determined by ^{1}H NMR analysis (Figures S1−S3) and the results are presented in Figure 1b. Primary alcohols butanol **A1** and benzyl alcohol **A3** displayed similar reactivities with αCC conversions of 78 and 69% in 2 h, respectively (Figure 1). The secondary alcohol **A2** presented a lower reactivity with a αCC conversion of 15% after 2 h. The lower reactivity of cyclohexanol was assigned to the steric hindrance around the alcohol group.

We then considered the reactions at a higher temperature (80 °C) in order to accelerate the conversion of αCC (Table 1; Figures S4−S6 in the Supporting Information). With **A1** and **A3**, αCC was selectively and almost quantitatively (>98%) converted into their corresponding oxo-carbonate **1** in a very short period of time, 15 min (Table 1, entries 1 and 9). The secondary alcohol **A2** still reacted slowly but faster compared to the same reaction carried out at 25 °C (with αCC conversion of 59% in 15 min at 80 °C; Table 1, entry 5). When the reaction time was extended further for **A2**, the corresponding oxo-carbonate **1** was selectively and quantitatively produced with no side product being identified even after 48 h at 80 °C. Importantly, despite the αCC ring-opening reaction being complete with **A3** after 15 min at 80 °C, maintaining this temperature for a longer period of time (up to 48 h) was detrimental to the selectivity of the reaction. Indeed, trace amounts of tetrasubstituted ethylene carbonate **2**, dibenzyl carbonate **3**, and hydroxyketone **4** were observed after 2 h. Moreover, the content of these side products increased substantially with the reaction time to reach 38% of **2**, 10% of **3**, and 12% of **4** after 48 h. The yield of oxo-carbonate **1** was thus decreased to 40%, while it was 99% after 15 min of reaction with **A3**. No side product was noted for the reaction of αCC with **A1**, even after 48 h at 80 °C. Note that the NMR structural identification of products **1**−**4** was confirmed by comparison of the GC−MS analysis results of the crude reaction mixture (**A3** + αCC with DBU for 48 h at 80 °C) (Figures S7−S11) with those of their commercially available or isolated reference samples (Figures S12−S16).

These observations suggested that the side products observed for the reaction of αCC with **A3** were formed by rearrangement of oxo-carbonate **1**. In order to give some clues to this hypothesis, this oxo-carbonate **1** was purified, isolated, solubilized in DMSO, and added with DBU (5 mol %) in the

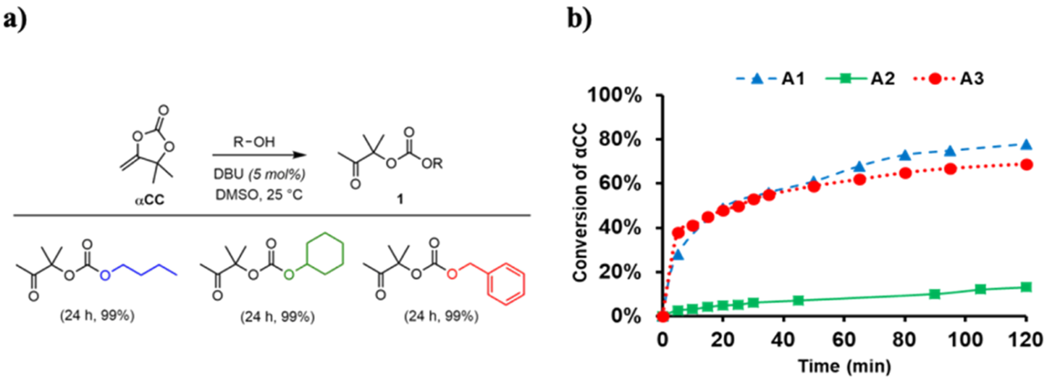

Figure 1. DBU-catalyzed alcoholysis of αCC with 1-butanol **A1**, cyclohexanol **A2**, or benzyl alcohol **A3** at 25 °C. (a) Reaction scheme and product yields after 24 h; (b) conversion of αCC vs time. Conditions: αCC (4 mmol), alcohol (4 mmol), and DBU (0.2 mmol) in dry DMSO (1 mL) at 25 °C under a nitrogen atmosphere.

Table 1. Alcoholysis of Exovinylene Cyclic Carbonate with 1-Butanol A1, Cyclohexanol A2, and Benzyl Alcohol A3 at 80 °C

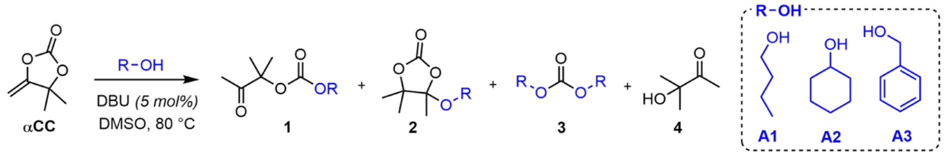

entry	R-OH	time	Conv$_{\alpha CC}$ [%]	yield 1 [%][a]	yield 2 [%][a]	yield 3 [%][a]	yield 4 [%][a]
1	A1	15 min	98	98	0	0	0
2		2 h	>99	>99	0	0	0
3		24 h	>99	>99	0	0	0
4		48 h	>99	>99	0	0	0
5	A2	15 min	59	59	0	0	0
6		2 h	89	89	0	0	0
7		24 h	>99	>99	0	0	0
8		48 h	>99	>99	0	0	0
9	A3	15 min	>99	>99	0	0	0
10		2 h	>99	94	3	2	1
11		24 h	>99	56	25	8	11
12		48 h	>99	40	38	10	12

[a] Yield determined by ^{1}H NMR spectroscopy on the crude product. Conditions: αCC (4 mmol), alcohol (4 mmol), and DBU (0.2 mmol) in dry DMSO (1 mL) at 80 °C under a nitrogen atmosphere.

Table 2. Rearrangement of Oxo-carbonate 1 (Prepared from αCC and A3) at 80 °C in the Presence or Absence of Additional A3

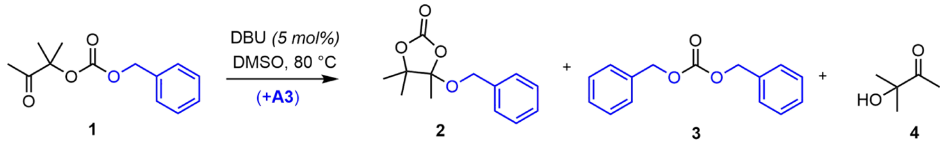

entry	R-OH	time (h)	Conv.1 [%]	yield 2 [%][a]	yield 3 [%][a]	yield 4 [%][a]
1	no	6	21	62	19	19
2		24	42	58	19	23
3[b]	A3	6	70	72	16	12
4[b]		24	88	60	23	17

[a] Yield determined by ^{1}H NMR spectroscopy of the crude product. [b] Reaction conducted in the presence of **A3** (0.5 equiv vs **1**). Conditions: oxo-carbonate **1** (4.06 mmol), DBU (0.203 mmol) in dry DMSO (1 mL) at 80 °C under a nitrogen atmosphere.

Scheme 3. Mechanism of Formation of Tetrasubstituted Ethylene Carbonate 2 by Addition of Benzyl Alcohol to αCC

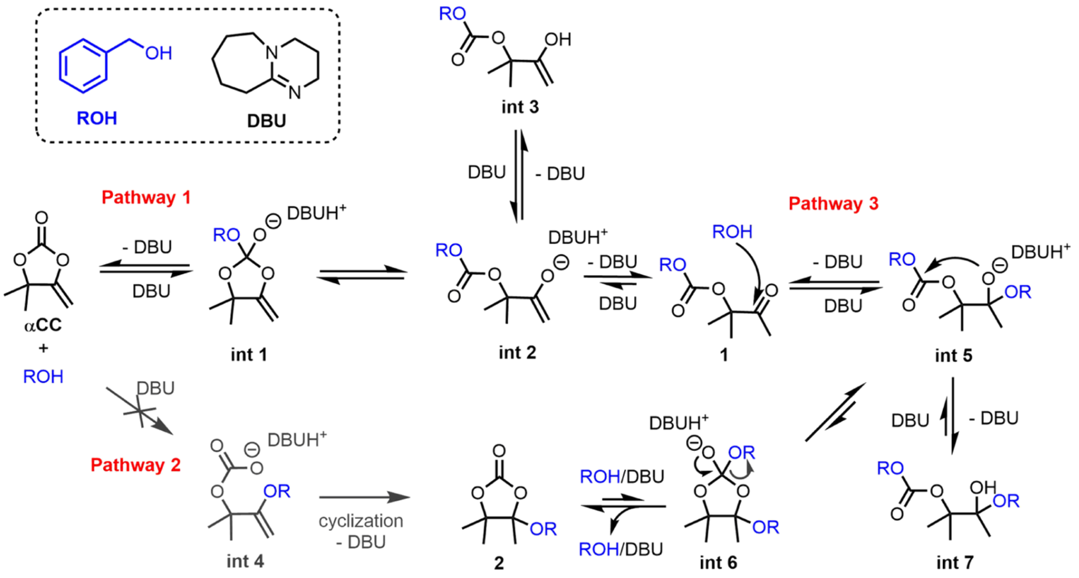

presence or absence of **A3** (0.5 equiv vs **1**). Table 2 shows the results. In both cases, the oxo-carbonate **1** was converted into tetrasubstituted ethylene carbonate **2** as the major product and into dibenzyl carbonate **3** and hydroxyketone **4** as the minor

Scheme 4. Gibbs-Free Energy Profile with the Corresponding Reaction Scheme and Transition-State Structures for Pathway 1 (p1) with the Formation of Oxo-carbonate 1 and for Pathway 3 (p3) with the Formation of Tetrasubstituted Ethylene Carbonate 2[a]

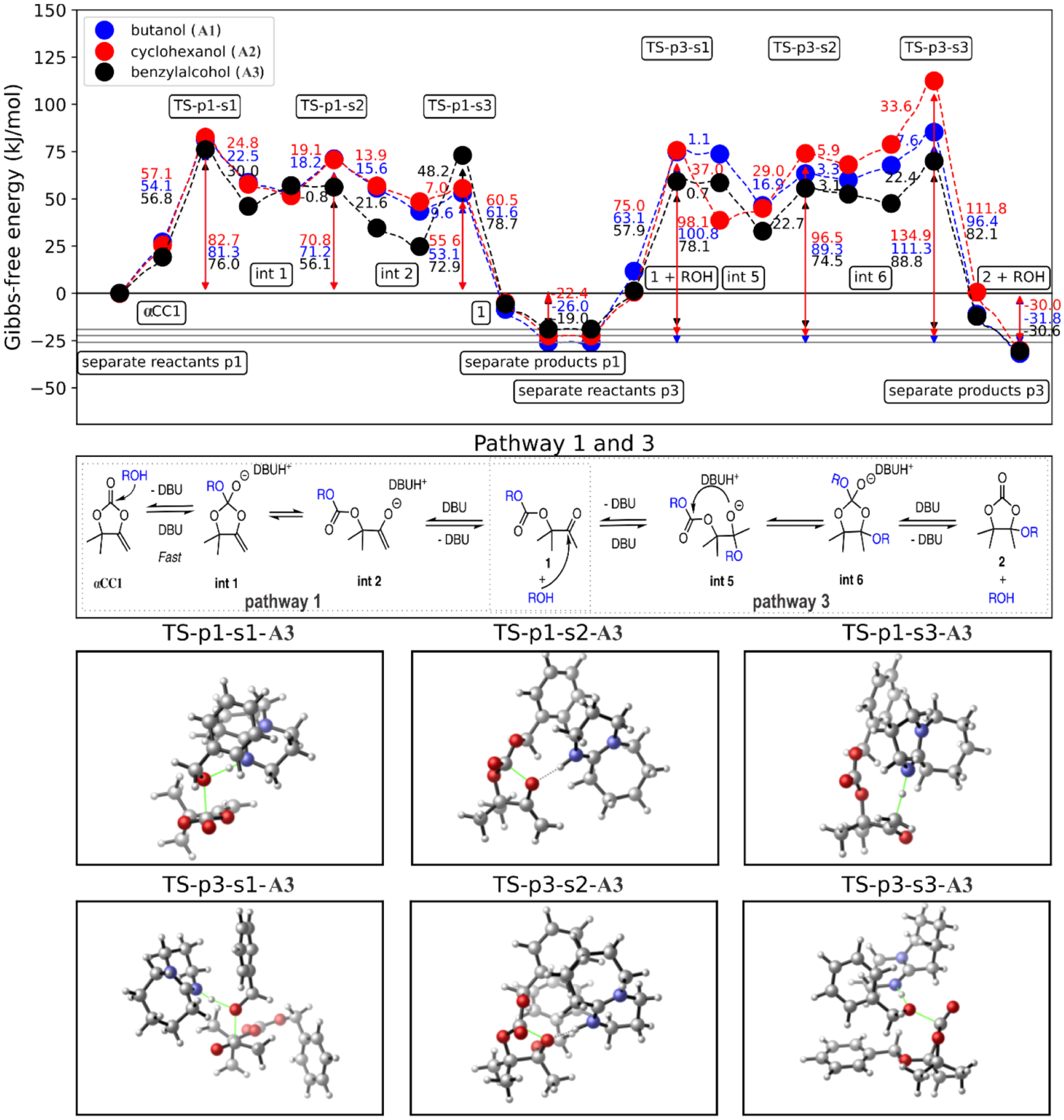

[a]The separate reactants for p3 are rescaled to the separate product of p1. Green bonds in the TS figures indicate bonds which are broken or formed. Energies in kJ·mol^{-1} (ωB97-XD/6-311++G**, IEFPCM (ϵ = 46.826), 298 K, 1 atm).

ones. The conversion of **1** increased with the reaction time, with a faster reaction noted in the presence of benzyl alcohol **A3**. Therefore, these experiments demonstrate that the formation of products **2**–**4** originated from a rearrangement of **1** and was accelerated by the addition of benzyl alcohol. The origin of these side products is of prime importance because these side reactions are expected to affect the polymer molar mass and microstructure. A thorough mechanistic investigation has therefore been performed in the next section.

Mechanistic Insight into the Alcoholysis of Exovinylene Cyclic Carbonate. Tetrasubstituted ethylene carbonates were identified by Costa et al. when αCC was generated *in situ* by the reaction of a propargylic alcohol with CO_2 in the presence of allyl alcohol or phenol catalyzed by superbases (7-methyl-1,5,7-triazabicyclo[4.4.0]dec-5-ene or 1,5,7-triazabicyclo[4.4.0]dec-5-ene) at 100 °C.[28] These side products were also observed by He et al. for similar reactions when phenol or allyl alcohol was substituted by benzyl alcohol in the presence of a silver salt (Ag_2CO_3/PPh_3) catalyst.[29] Although it was suggested that they might be formed by tautomerization of oxo-carbonate **1** and/or the addition of alcohol to the unsaturated double bond of αCC, the authors refrained from proposing any reaction mechanism.

https://dx.doi.org/10.1021/acssuschemeng.0c07683
ACS Sustainable Chem. Eng. XXXX, XXX, XXX−XXX

Our experimental results presented in Table 1 indicate that only benzyl alcohol (**A3**) is able to form some tetrasubstituted ethylene carbonate **2**, while butanol (**A1**) and cyclohexanol (**A2**) only furnished the corresponding oxo-carbonates **1**, at least under the investigated conditions. In order to gain an insight into the origin of this reaction and to understand the importance of the structure of the alcohol on the reaction selectivity, density functional theory (DFT) calculations based on static and molecular dynamics simulations were performed (Supporting Information, Section S3).

One may suggest that the formation of tetrasubstituted ethylene carbonate **2** follows a similar reaction pathway as that used for the addition of thiols to αCC:[19] fast reversible formation of oxo-carbonate **1** by the DBU-catalyzed ring opening of αCC by benzyl alcohol (Scheme 3: pathway 1 and Supporting Information, Section S3.2.2) with the concomitant slow and irreversible addition of alcohol to the disubstituted C═C double bond forming tetrasubstituted ethylene carbonate **2** (Scheme 3: pathway 2 and Supporting Information, Section S3.2.3). However, our theoretical calculations suggest an alternative more favorable pathway for the formation of **2** starting from oxo-carbonate **1** (Scheme 3: pathways 1 and 3). Compound **1** reacts with benzyl alcohol (**A3**) that is also liberated through the reversible reaction from the carbonate. In these calculations, we accounted for the DBU catalyst and the solvent environment implicitly in the static simulations and explicitly for all intermediates in the MD simulations, respectively (Supporting Information, Section S3.1). The stability of various intermediates under operating conditions, and thus, the formation of **int 3** and **int 7** is more thoroughly discussed in the Supporting Information.

The free energy profile of the reaction (pathways 1 and 3) is shown in Scheme 4. A key feature is the acidic strength of alcohols with their pK_a values that are sufficiently high to disfavor the formation of the corresponding salt (alkoxide). Instead, alcohol and DBU form a strong hydrogen-bonded complex (Figure S18), which facilitates the subsequent reactions. Regular MD simulations of the reactant complex confirm this as they show that this hydrogen-bonded complex, and not the corresponding salt, dominates the reactant region (Supporting Information, Section S3.2.1). Furthermore, salt formation is not observed in any of the static calculations.

As shown in Scheme 4, the rate-limiting step for the formation of oxo-carbonate **1** is the nucleophilic addition of alcohol to the carbonate carbonyl of αCC (TS-p1-s1) with apparent activation energies of 76.0, 81.3, and 82.7 kJ·mol^{-1} for benzyl alcohol **A3**, butanol **A1**, and cyclohexanol **A2**, respectively (in agreement with the experiments). This mechanism is triggered by the formation of a catalyst–alcohol ion-pair complex with immediate (rate-limiting) attack of alcohol on the neighboring αCC. Based on the relative differences in the activation energies of different alcohols, which are <10 kJ·mol^{-1}, the oxo-carbonate **1** formation should occur for all alcohols used, which is confirmed experimentally (Table 1). The reverse apparent reaction barriers amount to 91.9, 79.1, and 78.0 kJ·mol^{-1} for **A1**, **A3**, and **A2**, respectively. Reverse activation energies are hence within the same order of magnitude as the forward one, which suggests the reversibility of this pathway.

Noteworthy is the presence of π–cation and π-induced dipole interactions between the catalyst DBU-H$^+$ and benzyl alcohol **A3**, which is (obviously) not present for **A1** and **A2** (Scheme 4 and Figure 2a,b). These interactions substantially lower the activation barrier for the formation of **int 2** (or hence for the reverse reaction) and have a strong stabilizing effect on this intermediate in contrast to the stability of **int 2** for **A1** and **A2** (Scheme 4). To illustrate this, non-covalent interaction plots are shown in Figures 2a and 2b, which indicate that **int 2** is indeed much more stable due to the presence of stabilizing interactions between the benzylic moiety and DBU-H$^+$ which are completely absent for butanol (and cyclohexanol) featuring aliphatic chains. Additionally, for benzyl alcohol, a (spontaneous) equilibrium reaction is observed between **int 2** and **int 3**; this can hence directly influence the equilibria in which **int 2** is involved (Supporting Information, Section S3.2.2, Figure S21 simulation 1 and simulation 2). An increased stability of **int 1** and **int 2**, induced by interactions between the benzylic group and DBU-H$^+$, and the extra equilibria between **int 2** and **int 3** can directly influence the reaction kinetics for both the forward and reverse pathways (and hence the subsequent formation of tetrasubstituted ethylene carbonate **2**), which is not possible for **A1** and **A2**.

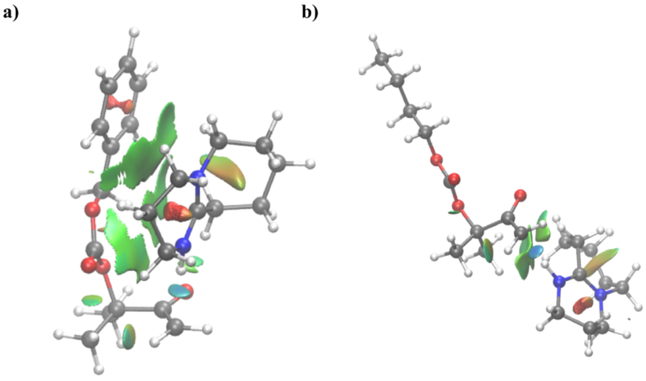

Figure 2. Non-covalent interaction plots for **int 2** with (a) benzyl alcohol and (b) butanol as the used alcohol. Green surfaces indicate weak vdW interactions, blue surfaces indicate strong stabilizing interactions (e.g., hydrogen bonding), and red surfaces indicate repulsive/destabilizing interactions.

Subsequently, as postulated by Lu et al.,[30] tetrasubstituted ethylene carbonate **2** can be formed through pathway 3 by a nucleophilic attack of a second alcohol molecule on the ketone of the formed oxo-carbonate **1**. This leads to the formation of **int 5** (Schemes 4 and 3, pathway 3), which is yet again the rate-determining step for this pathway. In contrast to pathway 1, we do observe significant differences for the rate-determining step of pathway 3 (>10 kJ·mol^{-1}) in line with the experimental results. Apparent activation energies for pathway 3, with respect to the separate reactants of pathway 3, are 78.1, 100.8, and 98.1 kJ·mol^{-1} for **A3**, **A1**, and **A2**, respectively. These barrier heights are in sharp contrast to the previously proposed pathway 2 (Supporting Information, Section S3.2.3, Scheme S2) as they are lowered by more than 50 kJ·mol^{-1}, showing that this new proposal is much more feasible. Furthermore, the trends for pathway 3 are in line with the experimental observations, which is not the case for pathway 2 (Supporting Information, Section S3.2.3, *vide infra*), that is, formation of tetrasubstituted ethylene carbonate is observed only for **A3**.

Intermediate stability is, similar to pathway 1, increased for benzyl alcohol, which can also be attributed to the induced π-type interactions. **Int 6** is clearly a metastable state which is prone to ring opening resulting in the formation of **int 5**. This metastability is also observed during the corresponding MD simulations (Supporting Information, Section S3.2.4, Figure S23). Scheme 4 further indicates that the tetrasubstituted ethylene carbonate **2** is thermodynamically favored and that the reverse reaction barrier is drastically higher than for pathway 1 shifting the equilibrium in favor of **2**. Additionally, it is noted throughout the static and dynamic simulations that the DBU positioning is highly determining for the stability (Supporting Information, Sections S3.2.2 and S3.2.4 and Figure 2).

To elaborate on the differences for the different alcohols, rate constants are calculated for the rate-limiting steps, and the results are presented in Table 3. Both for pathways 1 and 3, benzyl alcohol **A3** has increased rate constants compared to those of butanol **A1** and cyclohexanol **A2**, especially for the latter pathway a substantial increase is observed, that is 4 orders of higher magnitude with respect to **A1** and **A2**. More interesting to compare are the ratios of the rate constants which give an indication for the preference of each system to proceed along a certain pathway in case all reactants are present, that is, oxo-carbonate **1** formation has already occurred. For benzyl alcohol, both pathways are almost equally likely, in contrast to butanol and cyclohexanol which show a large preference (up to 3 orders of magnitude) for pathway 1. This can hence explain why, assuming that the reversibility of pathway 1 is feasible for all alcohols, no tetrasubstituted ethylene carbonate is observed for either butanol and cyclohexanol.

Table 3. Reaction Rates for the Rate-Determining Steps of Pathways 1 and 3 ($k_{1,p1}$ and $k_{1,p3}$, $M^{-2}\cdot s^{-1}$)[a]

alcohol	$k_{1,pathway1}$	$k_{1,pathway3}$	$k_{1,pathway1}/k_{1,pathway3}$
benzyl alcohol (**A3**)	3.05×10^{-1}	1.28×10^{-1}	2.4
butanol (**A1**)	3.58×10^{-2}	1.37×10^{-5}	2607.2
cyclohexanol (**A2**)	2.03×10^{-2}	3.98×10^{-5}	510.3

[a] Rate constants are calculated with respect to separate reactants or products. [ωB97-XD/6-311++G**, IEFPCM (ϵ = 46.826), 298 K, 1 atm].

As illustrated in Scheme 5, the side products **3** and **4** observed for the model reaction reported in Table 1 for **A3** can reasonably be obtained by the DBU-promoted transcarbonation of product **1** with benzyl alcohol as the α-hydroxyketone is a good leaving group, as also suggested by He et al.[29] In accordance with this, **3** and **4** are indeed formed in almost identical amounts. Assuming reactivity similar to pathway 1 for the different alcohols, the transcarbonation route is expected to proceed more easily for benzyl alcohol than for the aliphatic alcohols **A1** and **A2**.

Calculation of Parr functions enabled the elaboration of the difference in chemoselectivity of the alcohol attack on oxo-carbonate **1**, that is, its preferential addition to the ketone (C═O) (to form the tetrasubstituted ethylene carbonate **2**) or carbonate ((O)C═O) group (to form **3** and **4**) (Supporting Information, Sections S3.1.3 and S3.3). They showed that the formation of tetrasubstituted ethylene carbonate **2** is preferential over the transcarbonation route as C═O is more electrophilic than the carbonate site, and is therefore more prone to nucleophilic attack. This chemoselectivity is in line with the experimental results presented in Table 1.

From these modeling studies, it therefore appears that the formation of tetrasubstituted ethylene carbonate **2** proceeds through a nucleophilic attack of alcohol on the formed oxo-carbonate **1** (Scheme 3). This route explains the experimental observations and the difference in reactivity for the three different alcohols. Additionally, it is found that the DBU catalyst affects the intermediate stability. On one hand, it forms a strong hydrogen-bonded complex with the alcohol. On the other hand, for the specific combination of benzyl alcohol **A3** and DBU, it is shown that π-type interactions (e.g., cation−π, π−π, and π-induced dipole interactions) enable extra stabilization of various intermediates, which potentially increase the reaction rates. Finally, reactivity descriptors show the preference of the ketone group over carbonate toward nucleophilic attack, which explains the observed difference in yield for the tetrasubstituted ethylene carbonate **2** and the products **3** and **4** that result from the transcarbonation route.

Synthesis of Poly(oxo-carbonate)s by Polyaddition of BisαCCs with Biosourced Diols. A series of novel poly(β-oxo-carbonate)s were prepared by the polyaddition of two different CO_2-sourced bisαCC, that is, meso-4,4′-(ethane-1,2-diyl)bis(4-methyl-5-methylene-1,3-dioxolan-2-one) (**C1**) and 1,9-dimethylene-2,4,10,12-tetraoxodispiro[4.2.4^8.2^5]-tetradecane-3,11-dione (**C2**) with equimolar amounts of sugar-(1,4-butanediol **S1** or isosorbide **S2**) or lignin-derived (1,4-benzenedimethanol **L1** or *trans*-1,4-cyclohexanediol **L2**) diols (Scheme 6, Table 4). **S1** was here used as a benchmark diol.

Polymerizations at 25 °C. First, all copolymerizations were carried out at 25 °C using DBU as an organocatalyst (5 mol % compared to **C1** or **C2**) in dry DMSO (C = 0.78 M). For all PCs synthesized, the ^1H NMR spectra showed a full monomer consumption after 24 h. The copolymerization of *meso*-bisαCC **C1** and 1,4-butanediol (**S1**) or isosorbide (**S2**) was homogeneous during the reaction and gave poly(oxo-carbonate)s **C1S1** and **C1S2** with weight-average molar masses (M_w) of 26,700 and 9300 g/mol, respectively (Table 4, entries 1 and 2, Figure S24). Their characterization by ^1H and ^{13}C NMR spectroscopy gave clear insights into the formation of regioregular oxo-carbonate linkages and the absence of polymer defects (Figure 3). The ^1H NMR spectra highlighted the typical resonances of methylene of **C1S1** (δ =

Scheme 5. Chemoselectivity in the DBU-Catalyzed Addition of Alcohol to Oxo-carbonate

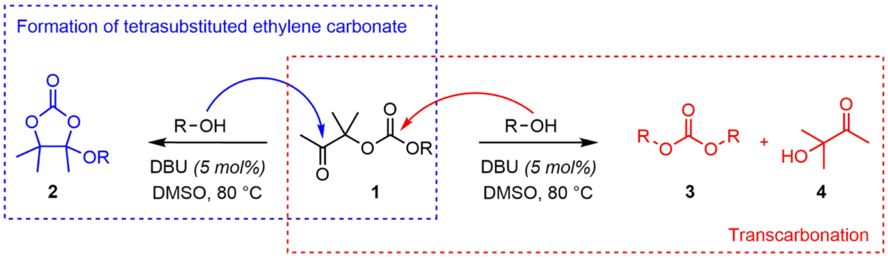

Scheme 6. Scope of Poly(oxo-carbonate)s Synthesized by Organocatalyzed Step-Growth Copolymerization of CO_2-Sourced bisαCCs with Bio-Based Diols

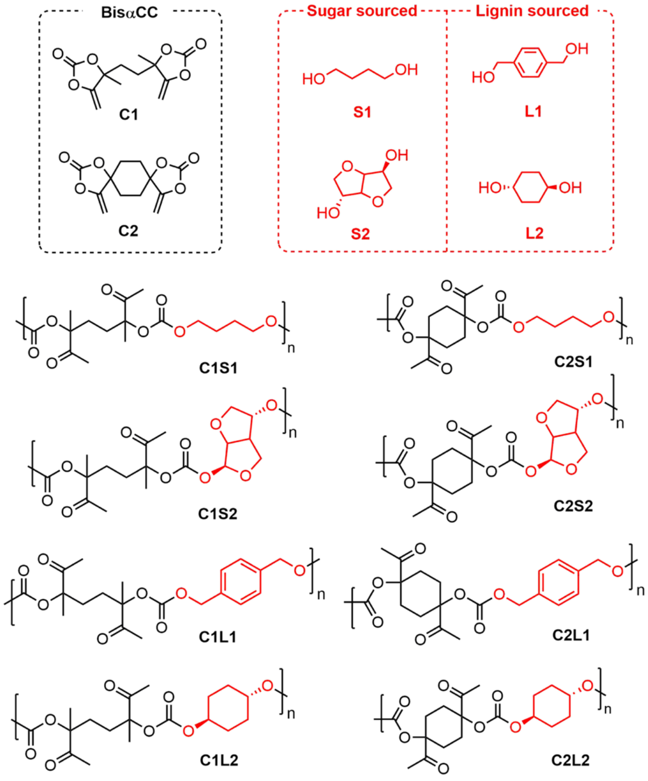

4.10 ppm) or methine of **C1S2** (δ = 5.01 ppm) adjacent to the oxo-carbonate linkages as well as signals at δ = 2.10−2.14 ppm from the methyl group of the pendant ketone moiety. The formation of oxo-carbonate linkages was further confirmed by the ^{13}C NMR resonances typical for the oxo and carbonate groups at δ = 206.0−206.5 ppm and δ = 152.9−153.6 ppm, respectively. Changing *meso*-bisαCC **C1** for *spiro*-bisαCC **C2** gave two new polymers, **C2S1** and **C2S2**, with different solubility behaviors (Table 4, entries 5 and 6). While **C2S2** displayed a M_w of 10,000 g/mol that remained soluble in DMSO during the course of the polymerization, **C2S1** precipitated during its formation and was found to be insoluble in all common organic solvents making the determination of its molar mass by SEC analysis impossible. ^{1}H and ^{13}C NMR spectra of **C2S2** gave the typical signatures of a regioregular poly(oxo-carbonate) (Figure 3). The microstructure of **C2S1** was elucidated by solid-state ^{13}C NMR spectroscopy that confirmed the formation of PC by the presence of ketone and carbonate signals at δ = 207.3 ppm and δ = 154.4 ppm, respectively (Figure S25).

The scope of poly(oxo-carbonate)s was extended to the copolymerization of **C1** or **C2** with the lignin-derived diols **L1** and **L2** (Table 4, entries 3, 4, 7, and 8). Initially, the medium was homogeneous, but the four PCs precipitated during their formation in DMSO. After 24 h, the polymers were isolated by filtration and found to be insoluble in the solvent used for SEC (DMF/LiBr or THF). However, **C1L1** and **C1L2** were found to be soluble in $CHCl_3$, and their molecular parameters were thus determined by SEC in $CHCl_3$. SEC analysis provided M_w of 13,600 g/mol for **C1L1** and 9400 g/mol for **C1L2** (Figure S26). Their ^{1}H and ^{13}C NMR spectra confirmed the formation of the corresponding regioregular poly(oxo-carbonate)s (Figure 3). As **C2L1** and **C2L2** were insoluble in many common organic solvents ($CHCl_3$, THF, DMF, DMSO, etc.), their structural characterization was only possible by solid-state ^{13}C NMR spectroscopy. Both **C2L1** and **C2L2** displayed the microstructure of a poly(oxo-carbonate) (Figure S27).

To attest for the microstructure of the polymers and get further insights into the nature of the chain-ends, the poly(oxo-carbonate) **C1S1** was selected for characterization by mass spectrometry (Figure 4). At first sight, a difference of 344 amu between each signal in the **C1S1** distributions confirms the presence of the corresponding oxo-carbonate units within the

Table 4. Poly(oxo-carbonate)s Synthesized by DBU-Catalyzed Step-Growth Copolymerization of bisαCCs with Various Diols at 25 °C: Molecular Characteristics and Thermal Properties[a]

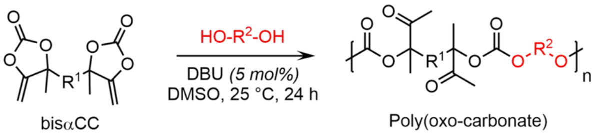

entry	polymer	M_n (g/mol)^{b}	M_w (g/mol)^{b}	$Đ^{b}$	$T_{deg,10\%}$ (°C)^{d}	T_g/T_m (°C)	X_c (%)^{i} at RT
1	**C1S1**	13,400	26,700	1.99	265	41/60^{e}	10
2	**C1S2**	4500	9300	2.06	256	88/--^{g}	0
3	**C1L1**	6000^{c}	13,600^{c}	2.24^{c}	216	71/84^{e}	8
4	**C1L2**	6000^{c}	9400^{c}	1.57^{c}	257	95/119^{e}	8
5	**C2S1**	^{h}	^{h}	^{h}	255	97/253^{f}	46
6	**C2S2**	6800	10,000	1.47	253	153/174^{e}	0
7	**C2L1**	^{h}	^{h}	^{h}	239	104/282^{f}	25
8	**C2L2**	^{h}	^{h}	^{h}	271	--/343^{f}	36

[a] Conditions: bisαCC (3.93 mmol), alcohol (3.93 mmol), DBU (0.196 mmol) in dry DMSO (5 mL) at 25 °C under a nitrogen atmosphere for 24 h. [b] Determined by SEC in DMF/LiBr. [c] Determined by SEC in $CHCl_3$. [d] Determined by TGA at 10% of weight loss. [e] Determined by FDSC analysis. The reported values of T_m were taken from the heating runs at 5000 K/s and after cooling the sample at 0.1 K/s. The reported values of T_g were taken from the heating runs at 1000 K/s and after cooling the sample at 4000 K/s. [f] Determined by FDSC analysis. The reported values of T_m and T_g were taken from the first scan at a heating rate of 20,000 K/s (to avoid degradation); The T_m values can be a mix between degradation and melting. [g] Determined by DSC analysis. [h] The polymer is insoluble in common organic solvents ($CHCl_3$, THF, DMF, or DMSO). [i] Degree of crystallinity of the powder from synthesis. The software Origin was employed to deconvolute WAXS patterns into amorphous and crystalline contributions, obtaining the degree of crystallinity by dividing the area under the crystalline peaks by the total area under the diffractogram.

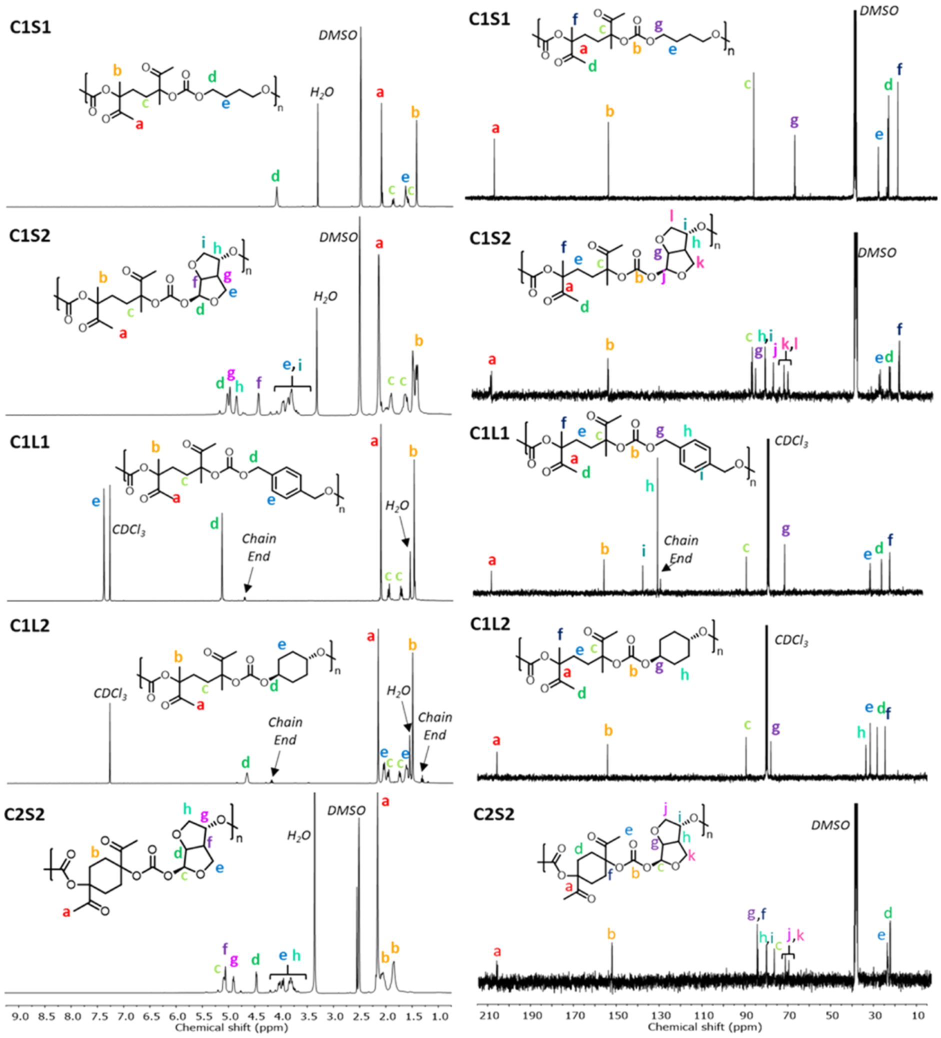

Figure 3. ^{1}H- and ^{13}C NMR characterization of poly(oxo-carbonate)s **C1S1** and **C1S2** (in DMSO-d_6), **C1L1** and **C1L2** (in $CDCl_3$), and **C2S2** (in DMSO-d_6).

polymers. Although the mass parameters (M_n or M_w) could not be determined due to the high molar-mass dispersity, the structural information also reveals that linear chains coexist with cyclic species (macrocyclic chains). The presence of macrocycles may arise from the end-to-end cyclization of the growing chains, as often observed in step-growth polymerization reactions.[31,32] **C1S1** displayed two types of chains with different end-groups. The most intense population is attributed to a linear poly(oxo-carbonate) terminated with butanediol units. The second linear distribution is associated with poly(oxo-carbonate) end-capped at one extremity by a hydroxyketone (e.g., m/z 3439.5), which may originate from the hydrolysis of the exovinylene chain-end upon MALDI characterization. It is also important to note that the cyclic species are mainly detected at low molecular weights and are probably overestimated.

Polymerizations at 80 °C. In order to accelerate the polymerizations and tentatively target PCs of higher molar masses, the polymerizations were carried out at 80 °C. For these studies, only *meso*-bis*α*CC **C1** was considered as it provided (at 25 °C) polymers that were soluble in common organic solvents and that could be characterized by liquid-state NMR spectroscopy and SEC analysis. For the sake of comparison, all experimental conditions were identical to the previous polymerizations, except for the temperature (80 vs 25 °C), and results are compared in Table 5. As determined by ^{1}H NMR spectroscopy for all PCs synthesized, **C1** was totally consumed after 24 h. When **C1** was copolymerized with **S1** or **L2**, polymers with oxo-carbonate linkages were obtained (Table 5, entries 1 and 3). No tetrasubstituted ethylene carbonate-type linkages were evidenced by ^{1}H NMR spectroscopy, at least within the detection limits of the technique (Figures S28 and S29, S30 and S31). These observations matched with our model reactions between *α*CC and **A1** or **A2** realized at 80 °C that did not reveal the formation of a 5-membered cyclic carbonate. Surprisingly, both **C1S1** and **C1L2** displayed significantly lower M_w compared to those measured for the same polymer produced at 25 °C. Indeed, **C1S1** prepared at 80 °C presented a M_w of 7000 g/mol at 80 °C (vs 26,700 g/mol at 25 °C) and **C1L2** a M_w of 7500 g/mol (vs 9400 g/mol at 25 °C) (entries 1 and 3, Table 5) (Figures S32 and S33). The transcarbonation reaction between the hydroxyl chain ends of the growing polymers and the oxo-carbonate linkages (that was favored at high temperatures, as demonstrated in the model reactions) was assumed to be responsible for the lower molar masses observed at 80 °C (Scheme 7). This side reaction left a polymer chain-end capped by an unreactive hydroxyketone and a polymer chain

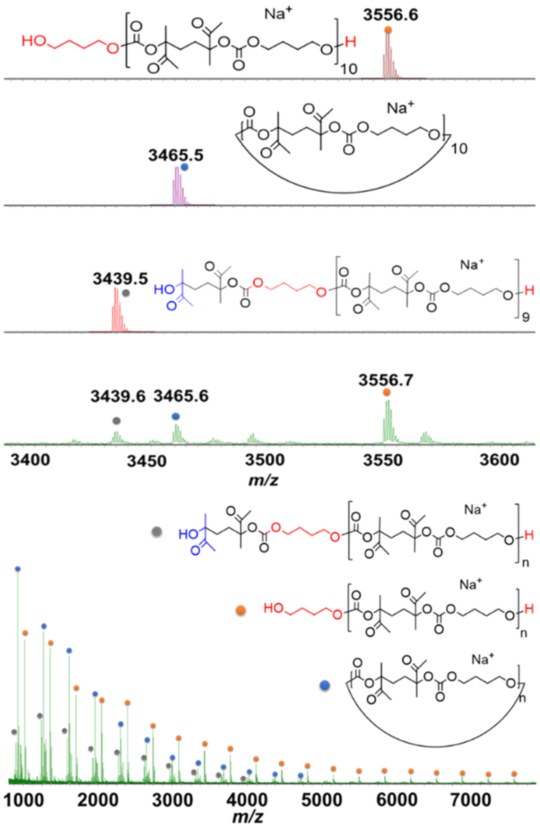

Figure 4. MALDI mass spectrum recorded for **C1S1**; the bottom part of the figure corresponds to the experimental mass spectrum, while the upper part is a magnification of the *m*/*z* area between 3400 and 3600 g/mol, showing a comparison between the experimental mass spectrum and the theoretical isotopic model.

bearing a new carbonate linkage. The presence of the hydroxyketone chain end was suggested by the presence of new singlets in the ^{1}H NMR spectra of **C1S1** or **C1L2** at 2.22 ppm (characteristic of a methyl group attached to an oxo group) and 1.30 ppm. The presence of a shoulder at 4.07 ppm (for **C1S1**) or 4.46 ppm (for **C1L2**) in the signals typical for the methylene or methine adjacent to the oxo-carbonate moieties attested the new carbonate linkage resulting from this transcarbonation reaction. By comparison of the relative intensities of peaks at 2.22 and 2.10 ppm, one quantified the level of the carbonate defect to 4% for **C1S1** and 6% for **C1L2**.

The occurrence of the transcarbonation side reaction on the polymer molar mass was further illustrated by carrying out three identical polymerizations of **C1** with **S1** at 80 °C and by stopping them at different periods of time (1, 6, and 24 h). The results are presented in Table S4 (Supporting Information). It comes out that the comonomers were rapidly consumed at the early stage of the reaction, giving the formation of a polymer of moderate molar mass (M_w = 10,000 g/mol after 1 h). However, with the reaction time, the polymer molar mass was decreased to 5800 g/mol after 24 h due to the occurrence of the transcarbonation reaction. This polymer molar mass is also illustrated in Figure S34 with the SEC chromatograms that shifted toward lower molar mass values with the reaction time. The transcarbonation was, however, slow and long reaction times were needed to observe the structural defects on the polymer.

When **C1** was copolymerized with **L1**, a polymer with a low M_w of 3500 g/mol (vs 13,600 g/mol at 25 °C) was synthesized after 24 h (Table 5, entry 2, Figure S35). Here also, PCs terminated by the hydroxyketone moiety and bearing some carbonate defects originating from the transcarbonation reaction were observed at a content of 8%. In contrast to the two previous examples, one also noticed the formation of additional five-membered cyclic carbonate linkages within the polymer microstructure with a content of 12%, as determined by ^{1}H NMR spectroscopy (Figure S36), in accordance with the model reactions with benzyl alcohol. Indeed, new methylene and methyl resonances of a tetrasubstituted ethylene carbonate unit were detected at 4.50, 1.63, and 1.45 ppm. The formation of these cyclic carbonate moieties was further corroborated by ^{13}C NMR spectroscopy by a new carbonyl signal at 145.0 ppm, two quaternary carbons at 82.3 and 108.2 ppm, and two methyl peaks attached to the carbonate cycle at 23.1 and 26.0 ppm (Figure S37).

Conclusively, structural defects were generated within the PC backbone when polymerizations were carried out at 80 °C, at least for long reaction times. They resulted from a slow transcarbonation reaction that furnished carbonate defect linkages and end-capped hydroxyketone PCs. In some cases (with 1,4-benzenedimethanol), an additional side reaction occurred by the slow addition of alcohol to the ketone group of the oxo-carbonate followed by cyclisation, forming a cyclic carbonate linkage in line with the observations made on the model reactions.

Thermal Properties of Poly(oxo-carbonate)s. The thermal properties of all defect-free poly(oxo-carbonate)s prepared at 25 °C were evaluated by TGA, standard DSC, and differential fast scanning calorimetry (FDSC), whose results are summarized in Table 4. The thermal degradation profiles of PCs are illustrated in Figure S38. The four polymers **C1S1**, **C1S2**, **C2S1**, and **C2S2** displayed moderate thermal stabilities with decomposition temperatures at 10% weight loss, $T_{d10\%}$, between 255 and 265 °C. Copolymers made from **L2** showed thermal stability in the same range of temperature with a $T_{d10\%}$ of 257 and 271 °C, respectively, for **C1L2** and **C2L2**. Changing the aliphatic diols by the aromatic diol **L1** led to polymers **C1L1** and **C2L1** with lower thermal stability, as attested by $T_{d10\%}$ of 216 and 239 °C. PCs containing the aromatic group also left some char at 600 °C (6 wt % for **C1L1** and 14 wt % for **C2L1**), whereas all other aliphatic PCs were almost completely decomposed at this temperature.

Remarkably, all poly(oxo-carbonate)s reported in Table 4 were able to crystallize (except for the sample **C1S2** that remained amorphous), as indicated by the reported melting point values. The glass-transition temperature (T_g) and the melting temperature (T_m) of the semicrystalline PCs were determined by standard DSC and FDSC. FDSC was employed to quench semi-crystalline samples employing cooling rates of 4000 °C/s. In this way, the fastest crystallizing samples were either quenched to the amorphous state or their crystallinities were substantially reduced. The T_g could therefore be easily determined during a subsequent heating scan. When the melting point of the sample was higher than 200 °C, the FDSC was used to heat the sample at 20,000 °C/s to avoid degradation as much as possible and still detect the melting endotherm.

From the copolymer series illustrated in Table 4, **C1S2** made from *meso*-bisαCC and isosorbide was amorphous with only a T_g at 88 °C (Figure S39). All the other samples were

Table 5. Comparison of the Structure of the Carbonate Linkages and Macromolecular Characteristics of the PCs Prepared by DBU-Catalyzed Copolymerization of bisαCCs with Diols at 25 and 80 °C in dry DMSO[a]

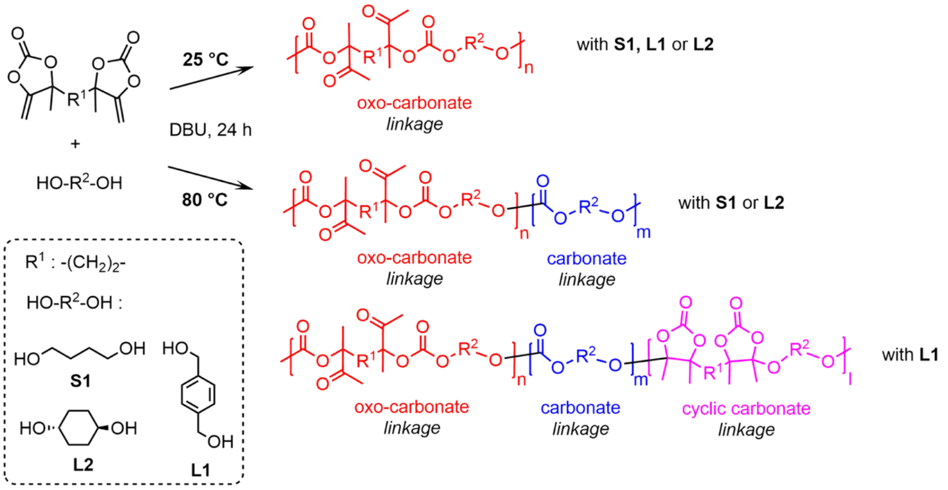

entry	polymer	T (°C)	Conv. C1 (%)	oxo-carbonate linkage (%)	cyclic carbonate linkage (%)	carbonate linkage (%)	M_n (g/mol)[b]	M_w (g/mol)[b]	Đ[b]
1	**C1S1**	25	>99	100	0	0	13,400	26,700	1.99
		80	>99	96	0	4	3800	7000	1.84
2	**C1L1**	25	>99	100	0	0	6000[c]	13,600[c]	2.24[c]
		80	>99	80	12	8	1900[c]	3500[c]	1.83[c]
3	**C1L2**	25	>99	100	0	0	6000[c]	9400[c]	1.57[c]
		80	>99	94	0	6	3300[c]	7500[c]	2.25[c]

[a] Conditions: bisαCC (3.93 mmol), alcohol (3.93 mmol), DBU (0.196 mmol) in dry DMSO (5 mL) at 25 or 80 °C, under a nitrogen atmosphere. [b] Determined by SEC in DMF/LiBr. [c] Determined by SEC in $CHCl_3$.

Scheme 7. Transcarbonation Reaction between the Hydroxyl Chain Ends of the Growing Polymers and the Oxo-carbonate Linkages

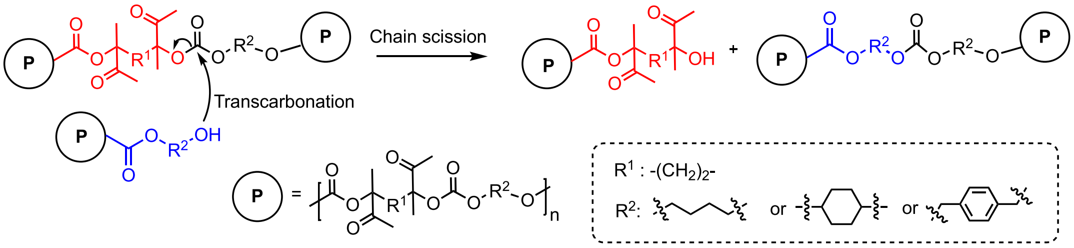

semi-crystalline, and their T_g and T_m values are reported in Table 4 (Figures S40–S46). Based on their chemical structures illustrated in Scheme 6, a close correlation was found between the high values of T_g/T_m transitions and the chain rigidity in most cases, as expected.

Figure 5 shows the WAXS diffractograms of selected samples. The presence of well-defined diffraction peaks confirmed the semi-crystalline character of the samples. Their crystallinities were estimated by deconvoluting the areas of the WAXS patterns into amorphous and crystalline contributions. Then, the degree of crystallinity was obtained by dividing the area under the crystalline peaks by the total area under the diffractogram. Crystallinity values varied from 8% for the less crystalline **C1L2** sample to 46% for the most crystalline **C2S1** sample (entries 4 and 5, Table 4). The crystalline structure of the novel poly(oxo-carbonate)s prepared here is unknown, so we cannot assign the reflections to the crystallographic planes that originate them. Establishing the crystalline structure of polymers is, however, beyond the scope of the present paper. Nevertheless, judging by the

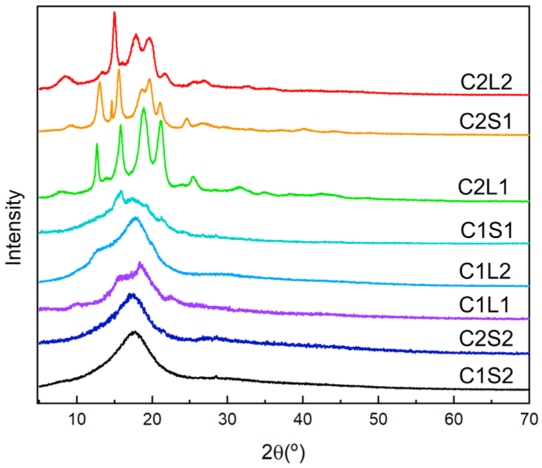

Figure 5. WAXS patterns taken at room temperature of poly(oxo-carbonate)s.

changes in diffraction angles and their corresponding distances (Supporting Information, Table S5), the polymers all crystallized in different types of unit cells, as their chemical structure varies significantly from one another, and hence, in molecular chain packing within their respective crystalline structures.

■ CONCLUSIONS

The emergence of CO_2-sourced exovinylene bicyclic carbonates (bisαCCs) in polymer science prompted us to investigate the scope and limitations of their organocatalyzed step-growth copolymerization with biorenewable diols to PCs. Model reactions were first carried out on small molecules in order to understand the structural influence of alcohols, the temperature (25 or 80 °C), and the use of an organocatalyst (DBU) on the rate of cyclic carbonate ring-opening and product selectivity. Based on these studies, a series of regioregular and defect-free poly(oxo-carbonate)s of different structures and reasonable molar masses (M_w up to 26,700 g/mol) were prepared at 25 °C using sugar- (1,4-butanediol and isosorbide) or lignin-derived (1,4-benzenedimethanol and 1,4-cyclohexanediol) diols and two different CO_2-sourced bis-αCCs. By performing the polymerizations at 80 °C, structural defects were, however, introduced within the poly(oxo-carbonate) chains, that is, a second type of carbonate linkage originated from transcarbonation reactions in all cases. When 1,4-benzenedimethanol was used, an additional side reaction was noted and provided tetrasubstituted ethylene carbonate linkages. These side reactions observed at 80 °C limited the polymer molar mass for long reaction times. The mechanism of formation of these side reactions was considered by DFT modeling on model compounds. It was found that the tetrasubstituted ethylene carbonate linkage proceeded through a nucleophilic attack of the alcohol on the ketone group of the formed oxo-carbonate, inducing cyclization. Importantly, the DBU catalyst influenced the intermediate stability. It formed a strong hydrogen-bonded complex with the alcohol and, for the specific combination of benzyl alcohol (a model compound of 1,4-benzenedimethanol) and DBU, π-type interactions (e.g., cation−π, π−π, and π-induced dipole interactions) were noted and enabled extra stabilization of various intermediates, which potentially increased the reaction rates. Finally, reactivity descriptors enabled explaining the observed difference in yield for the tetrasubstituted ethylene carbonate linkage and the linear carbonate (originating from transcarbonation).

Finally, the thermal properties of poly(oxo-carbonate)s designed at 25 °C were evaluated by thermogravimetry (TGA), standard DSC, and FDSC. Depending on their microstructures, poly(oxo-carbonate)s presented a degradation temperature between 216 and 271 °C. With the exception of one poly(oxo-carbonate) made from isosorbide that was amorphous with a glass-transition temperature (T_g) of 88 °C, all the other PCs were semi-crystalline with a melting temperature (T_m) ranging from 60 to 343 °C. Preliminary WAXS studies confirmed the ability of these PCs to crystallize.

This work highlights the potential of this process for the facile preparation of PCs using diols and carbon dioxide as bioresources under mild reaction conditions and shows how the polymer linkages can be modified by the experimental conditions. The fraction of biorenewables (CO_2 + diol) incorporated in the polymers is high (50−60 wt %), attesting for the importance of the process for the more sustainable production of plastics. The level of sustainability of these materials might be further increased by proposing greener routes to producing bisαCCs. Indeed, their current synthesis uses petro-based diones (1,4-cyclohexanone or 2,5-hexanedione in this work) and Grignard's reagent (ethynyl magnesium bromide) to prepare the propargylic alcohols needed for coupling to CO_2. Bio-based approaches might consist of starting from 1,4-cyclohexanone prepared from succinic acid[33] or 2,5-hexanedione obtained by the hydrolysis of sugar-derived 2,5-dimethylfuran.[34,35] Grignard reagents will still have to be used; however, bispropargylic alcohols might be easily obtained from calcium carbide as the acetylene source.[36,37]

■ ASSOCIATED CONTENT

Supporting Information

The Supporting Information is available free of charge at https://pubs.acs.org/doi/10.1021/acssuschemeng.0c07683.

> ^{1}H and ^{13}C NMR spectra of model compounds and polymers; GC-FID and MS spectra of model reactions; DFT calculations of the side reaction and DFT protocols; and SEC chromatograms, TGA curves, and DSC and FDSC curves of polymers (PDF)

■ AUTHOR INFORMATION

Corresponding Authors

Veronique Van Speybroeck − *Center for Molecular Modeling, University of Ghent, 9052 Zwijnaarde, Belgium;* orcid.org/0000-0003-2206-178X; Email: veronique.vanspeybroeck@ugent.be

Bruno Grignard − *Center for Education and Research on Macromolecules (CERM), CESAM Research Unit, University of Liège, 4000 Liege, Belgium;* orcid.org/0000-0002-6016-3317; Email: bruno.grignard@uliege.be

Christophe Detrembleur − *Center for Education and Research on Macromolecules (CERM), CESAM Research Unit, University of Liège, 4000 Liege, Belgium;* orcid.org/0000-0001-7849-6796; Email: christophe.detrembleur@uliege.be

Authors

Fabiana Siragusa − *Center for Education and Research on Macromolecules (CERM), CESAM Research Unit, University of Liège, 4000 Liege, Belgium*

Elias Van Den Broeck − *Center for Molecular Modeling, University of Ghent, 9052 Zwijnaarde, Belgium;* orcid.org/0000-0002-9609-4333

Connie Ocando − *POLYMAT and Faculty of Chemistry, University of the Basque Country UPV/EHU, 20018 Donostia-San Sebastián, Spain;* orcid.org/0000-0003-4123-1879

Alejandro J. Müller − *POLYMAT and Faculty of Chemistry, University of the Basque Country UPV/EHU, 20018 Donostia-San Sebastián, Spain; IKERBASQUE, Basque Foundation for Science, Bilbao 48013, Spain;* orcid.org/0000-0001-7009-7715

Gilles De Smet − *Organic Synthesis Division, Department of Chemistry, University of Antwerp, 2020 Antwerp, Belgium*

Bert U. W. Maes − *Organic Synthesis Division, Department of Chemistry, University of Antwerp, 2020 Antwerp, Belgium;* orcid.org/0000-0003-0431-7606

Julien De Winter − *Mass Spectrometry Research Group, Interdisciplinary Center of Mass Spectrometry (CISMa),* *University of Mons, 7000 Mons, Belgium;* orcid.org/0000-0003-3429-5911

Complete contact information is available at:
https://pubs.acs.org/10.1021/acssuschemeng.0c07683

Notes

The authors declare no competing financial interest.

ACKNOWLEDGMENTS

The authors from Liege, Ghent, and Antwerp thank the "Fonds National pour la Recherche Scientifique" (F.R.S.-FNRS) and the Fonds Wetenschappelijk Onderzoek—Vlaanderen (FWO) for financial support in the frame of the EOS project no. O019618F (ID EOS: 30902231). The authors from Liege thank the CESAM Research Unit for financial support and Dr. Olivier Coulembier (University of Mons, Belgium) for SEC analyses of $CHCl_3$. C.O. acknowledges "Diputación Foral de Gipuzkoa" in the framework program "Fellows Gipuzkoa de Atracción y Retención de Talento". The authors thank for the technical and human support provided by SGIker (UPV/EHU/ERDF, EU), in particular, to the general X-ray service of the UPV/EHU: Molecules and Material unit. C.D. is the F.R.S.-FNRS Research Director. B.U.W.M. thanks the Francqui Foundation for appointment as the Collen-Francqui professor. The computational resources and services used were provided by Ghent University (Stevin Supercomputer Infrastructure), the VSC (Flemish Supercomputer Center), funded by the Research Foundation—Flanders (FWO). This work was supported by the Research Board of the Ghent University (BOF). The UMONS MS laboratory acknowledges F.R.S.-F.N.R.S. for its contribution to the acquisition of the Waters QToF Premier mass spectrometer and for continuing support.

REFERENCES

(1) Kyriacos, D. *Polycarbonates*; Elsevier Ltd, 2017.

(2) Fukuoka, S.; Tojo, M.; Hachiya, H.; Aminaka, M.; Hasegawa, K. Green and Sustainable Chemistry in Practice: Development and Industrialization of a Novel Process for Polycarbonate Production from CO_2 without Using Phosgene. *Polym. J.* **2007**, *39*, 91−114.

(3) Kim, W. B.; Joshi, U. A.; Lee, J. S. Making Polycarbonates without Employing Phosgene: An Overview on Catalytic Chemistry of Intermediate and Precursor Syntheses for Polycarbonate. *Ind. Eng. Chem. Res.* **2004**, *43*, 1897−1914.

(4) Fukuoka, S.; Fukawa, I.; Adachi, T.; Fujita, H.; Sugiyama, N.; Sawa, T. Industrialization and Expansion of Green Sustainable Chemical Process: A Review of Non-Phosgene Polycarbonate from CO_2. *Org. Process Res. Dev.* **2019**, *23*, 145−169.

(5) Grignard, B.; Gennen, S.; Jérôme, C.; Kleij, A. W.; Detrembleur, C. Advances in the Use of CO_2 as a Renewable Feedstock for the Synthesis of Polymers. *Chem. Soc. Rev.* **2019**, *48*, 4466−4514.

(6) Tamura, M.; Ito, K.; Honda, M.; Nakagawa, Y.; Sugimoto, H.; Tomishige, K. Direct Copolymerization of CO_2 and Diols. *Sci. Rep.* **2016**, *6*, 24038.

(7) Huang, J.; Worch, J. C.; Dove, A. P.; Coulembier, O. Update and Challenges in Carbon Dioxide-Based Polycarbonate Synthesis. *ChemSusChem* **2020**, *13*, 469−487.

(8) Schutyser, W.; Renders, T.; Van Den Bosch, S.; Koelewijn, S.-F.; Beckham, G. T.; Sels, B. F. Chemicals from Lignin: An Interplay of Lignocellulose Fractionation, Depolymerisation, and Upgrading. *Chem. Soc. Rev.* **2018**, *47*, 852−908.

(9) Sun, Z.; Fridrich, B.; De Santi, A.; Elangovan, S.; Barta, K. Bright Side of Lignin Depolymerization: Toward New Platform Chemicals. *Chem. Rev.* **2018**, *118*, 614−678.

(10) Gong, Z.-J.; Li, Y.-R.; Wu, H.-L.; Lin, S. D.; Yu, W.-Y. Direct Copolymerization of Carbon Dioxide and 1,4-Butanediol Enhanced by Ceria Nanorod Catalyst. *Appl. Catal., B* **2020**, *265*, 118524−118536.

(11) Jiang, Z.; Chen, L.; Wenchun, X.; Gross, R. A. Controlled Lipase-Catalyzed Synthesis of Poly(Hexamethylene Carbonate). *Macromolecules* **2007**, *40*, 7934−7943.

(12) Meabe, L.; Lago, N.; Rubatat, L.; Li, C.; Müller, A. J.; Sardon, H.; Armand, M.; Mecerreyes, D. Polycondensation as a Versatile Synthetic Route to Aliphatic Polycarbonates for Solid Polymer Electrolytes. *Electrochim. Acta* **2017**, *237*, 259−266.

(13) Sun, J.; Kuckling, D. Synthesis of High-Molecular-Weight Aliphatic Polycarbonates by Organo-Catalysis. *Polym. Chem.* **2016**, *7*, 1642−1649.

(14) Naik, P. U.; Refes, K.; Sadaka, F.; Brachais, C.-H.; Boni, G.; Couvercelle, J.-P.; Picquet, M.; Plasseraud, L. Organo-Catalyzed Synthesis of Aliphatic Polycarbonates in Solvent-Free Conditions. *Polym. Chem.* **2012**, *3*, 1475−1480.

(15) Gennen, S.; Grignard, B.; Tassaing, T.; Jérôme, C.; Detrembleur, C. CO_2 -Sourced α-Alkylidene Cyclic Carbonates: A Step Forward in the Quest for Functional Regioregular Poly(Urethane)s and Poly(Carbonate)S. *Angew. Chem., Int. Ed.* **2017**, *56*, 10394−10398.

(16) Ouhib, F.; Meabe, L.; Mahmoud, A.; Eshraghi, N.; Grignard, B.; Thomassin, J.-M.; Aqil, A.; Boschini, F.; Jérôme, C.; Mecerreyes, D.; Detrembleur, C. CO_2 -Sourced Polycarbonates as Solid Electrolytes for Room Temperature Operating Lithium Batteries. *J. Mater. Chem. A* **2019**, *7*, 9844−9853.

(17) Gennen, S.; Grignard, B.; Jérôme, C.; Detrembleur, C. CO_2-Sourced Non-Isocyanate Poly(Urethane)s with PH-Sensitive Imine Linkages. *Adv. Synth. Catal.* **2019**, *361*, 355−365.

(18) Habets, T.; Siragusa, F.; Grignard, B.; Detrembleur, C. Advancing the Synthesis of Isocyanate-Free Poly(Oxazolidones)s: Scope and Limitations. *Macromolecules* **2020**, *53*, 6396−6408.

(19) Ouhib, F.; Grignard, B.; Van Den Broeck, E.; Luxen, A.; Robeyns, K.; Van Speybroeck, V.; Jerome, C.; Detrembleur, C. A Switchable Domino Process for the Construction of Novel CO_2 -Sourced Sulfur-Containing Building Blocks and Polymers. *Angew. Chem., Int. Ed.* **2019**, *58*, 11768−11773.

(20) Dabral, S.; Schaub, T. The Use of Carbon Dioxide (CO_2) as a Building Block in Organic Synthesis from an Industrial Perspective. *Adv. Synth. Catal.* **2019**, *361*, 223−246.

(21) Ouhib, F.; Meabe, L.; Mahmoud, A.; Grignard, B.; Thomassin, J.-M.; Boschini, F.; Zhu, H.; Forsyth, M.; Mecerreyes, D.; Detrembleur, C. Influence of the Cyclic versus Linear Carbonate Segments in the Properties and Performance of CO_2 -Sourced Polymer Electrolytes for Lithium Batteries. *ACS Appl. Polym. Mater.* **2020**, *2*, 922−931.

(22) Dabral, S.; Licht, U.; Rudolf, P.; Bollmann, G.; Hashmi, A. S. K.; Schaub, T. Synthesis and Polymerisation of α-Alkylidene Cyclic Carbonates from Carbon Dioxide, Epoxides and the Primary Propargylic Alcohol 1,4-Butynediol. *Green Chem.* **2020**, *22*, 1553−1558.

(23) Tounzoua, C. N.; Grignard, B.; Brege, A.; Jerome, C.; Tassaing, T.; Mereau, R.; Detrembleur, C. A Catalytic Domino Approach toward Oxo-Alkyl Carbonates and Polycarbonates from CO_2 , Propargylic Alcohols, and (Mono- and Di-)Alcohols. *ACS Sustain. Chem. Eng.* **2020**, *8*, 9698−9710.

(24) Kricheldorf, H. R. "Sugar Diols" as Building Blocks of Polycondensates. *J. Macromol. Sci., Chem.* **1997**, *37*, 599−631.

(25) Yu, Y.; Pang, C.; Jiang, X.; Yang, Z.; Ma, J.; Gao, H. Copolycarbonates Based on a Bicyclic Diol Derived from Citric Acid and Flexible 1,4-Cyclohexanedimethanol: From Synthesis to Properties. *ACS Macro Lett.* **2019**, *8*, 454−459.

(26) Burgard, A.; Burk, M. J.; Osterhout, R.; Van Dien, S.; Yim, H. ScienceDirect Development of a Commercial Scale Process for Production of 1 , 4-Butanediol from Sugar. *Curr. Opin. Biotechnol.* **2016**, *42*, 118−125.

(27) Grignard, B.; Ngassamtounzoua, C.; Gennen, S.; Gilbert, B.; Méreau, R.; Jerome, C.; Tassaing, T.; Detrembleur, C. Boosting the Catalytic Performance of Organic Salts for the Fast and Selective

Synthesis of α-Alkylidene Cyclic Carbonates from Carbon Dioxide and Propargylic Alcohols. *ChemCatChem* **2018**, *10*, 2584−2592.

(28) Ca', N. D.; Gabriele, B.; Ruffolo, G.; Veltri, L.; Zanetta, T.; Costa, M. Effective Guanidine-Catalyzed Synthesis of Carbonate and Carbamate Derivatives from Propargyl Alcohols in Supercritical Carbon Dioxide. *Adv. Synth. Catal.* **2011**, *353*, 133−146.

(29) Zhou, Z.-H.; Song, Q.-W.; Xie, J.-N.; Ma, R.; He, L.-N. Silver(I)-Catalyzed Three-Component Reaction of Propargylic Alcohols, Carbon Dioxide and Monohydric Alcohols: Thermodynamically Feasible Access to β-Oxopropyl Carbonates. *Chem.—Asian J.* **2016**, *11*, 2065−2071.

(30) Zhou, H.; Zhang, H.; Mu, S.; Zhang, W.-Z.; Ren, W.-M.; Lu, X.-B. Highly Regio- And Stereoselective Synthesis of Cyclic Carbonates from Biomass-Derived Polyols: Via Organocatalytic Cascade Reaction. *Green Chem.* **2019**, *21*, 6335−6341.

(31) Kricheldorf, H. R. Cyclic Polymers: Synthetic Strategies and Physical Properties. *J. Polym. Sci., Part A: Polym. Chem.* **2010**, *48*, 251−284.

(32) Josse, T.; De Winter, J.; Gerbaux, P.; Coulembier, O. Cyclic Polymers by Ring-Closure Strategies Angewandte. *Angew. Chem., Int. Ed.* **2016**, *55*, 13944−13958.

(33) Nielsen, A. T.; Carpenter, W. R. 1,4-Cyclohexanedione. *Org. Synth.* **1965**, *45*, 25.

(34) Nikbin, N.; Caratzoulas, S.; Vlachos, D. G. On the Brønsted Acid-Catalyzed Homogeneous Hydrolysis of Furans. *ChemSusChem* **2013**, *6*, 2066−2068.

(35) Li, Y.; Lv, G.; Wang, Y.; Deng, T.; Wang, Y.; Hou, X.; Yang, Y. Synthesis of 2,5-Hexanedione from Biomass Resources Using a Highly Efficient Biphasic System. *ChemistrySelect* **2016**, *1*, 1252−1255.

(36) Hosseini, A.; Seidel, D.; Miska, A.; Schreiner, P. R. Fluoride-Assisted Activation of Calcium Carbide: A Simple Method for the Ethynylation of Aldehydes and Ketones. *Org. Lett.* **2015**, *17*, 2808−2811.

(37) Sum, Y. N.; Yu, D.; Zhang, Y. Synthesis of Acetylenic Alcohols with Calcium Carbide as the Acetylene Source. *Green Chem.* **2013**, *15*, 2718−2721.